

Simulation tool for atmospheric aerosol nucleation bursts

H. Tammet¹ and M. Kulmala²

¹Institute of Environmental Physics, University of Tartu, Ülikooli 18, 50090 Tartu, Estonia

²Department of Physical Sciences, Division of Atmospheric Sciences,
P.O. Box 64, FIN-00014, University of Helsinki, Finland

Abstract. A numerical model for atmospheric aerosol nucleation bursts is presented as a tool for the analysis of measurements. It includes a minimum of physical assumptions and 94 user-controlled parameters. The model is based on computationally efficient parametrization of submodels, which allow considering the ion-induced and homogeneous nucleation, depletion of nanoparticles and ions on the pre-existing aerosol, the nano-Köhler growth function, the molecule-particle interception geometry, quantum retardation of sticking, the electric charges of particles, the molecular dipole moments, and the polarization interaction. The evolution of the size distribution is computed using a sectional model with several thousands of sections. Computing time on an ordinary PC is counted in seconds in case of a typical task with several thousands of time steps and several thousands of size sections.

Keywords: Aerosol dynamics; Atmospheric ions; Nucleation bursts; Numerical models

Nomenclature

B	mechanic mobility of ions or particles
d	diameter
d_b	average diameter of pre-existing background aerosol particles
d_q	characteristic length of Coulomb attachment
D	diffusion coefficient
e	elementary charge 1.6×10^{-19} C
f_{nK}	nano-Köhler factor of the growth rate
En	Nadykto-Yu enhancement factor
G	growth rate of particles
h	extra distance expressing the van der Waals interaction
I	ionization rate
J	nucleation rate
k	Boltzmann constant 1.38×10^{-23} J K ⁻¹
m	mass of ion or particle
n	concentration of ions
N	concentration of nucleation mode particles
N	concentration of pre-existing particles of background aerosol
N_e	concentration of elementary charges carried by background aerosol
p	sticking probability or power in nano-Köhler approximation
q	number of elementary charges on a particle (particle charge is qe)
r	distance from the center
s_n	sink of ions on nucleation mode aerosol (all sinks are measured in s ⁻¹)
s_b	sink of ions on background aerosol
S_b	sink of particles on background aerosol
t	time
T	absolute temperature
u	velocity
U	potential energy
V	volume

Z	electric mobility
α	dipole polarizability or ion-ion recombination coefficient
β_q	coefficient of attachment of a positive ion to a particle of charge qe
γ	ratio of fluxes calculated according to continuum and kinetic regime equations
δ	effective collision distance between centers of colliding spheres $\delta = 2\sqrt{\Omega/\pi}$
ϵ_0	electric constant $8.85 \times 10^{-12} \text{ F m}^{-1}$
κ	interpolation coefficient in the Sahni equation
μ	electric dipole moment
ρ	density of particulate matter
φ	flux of molecules or particles
Ω	collision integral

Introduction

Atmospheric aerosol has a crucial influence on the radiation balance of the Earth and it is the most vulnerable factor of climate. Knowledge of the genesis of atmospheric aerosol is limited due to the very small size of the newly born particles, which creates difficulties both in the experiment and theory. New particles are formed from gaseous admixtures of the air in a process called the homogeneous nucleation. Homogeneous nucleation in the atmospheric air often happens as a burst event that typically lasts for a few hours. Research on nucleation bursts has become as a promising method of learning about the mechanisms that control formation and growth of new particles in the Earth's atmosphere. The most reliable information about the atmospheric aerosol nucleation originates from measurements, which form the basis for examining of theoretical models that aspire to explain the physical and chemical mechanisms of homogeneous nucleation. An overview of problems and observations of the formation and growth of atmospheric aerosol particles is recently presented (Kulmala et al., 2004b).

The growth of newly born particles is described and simple conclusions about the parameters of nucleation and particle growth during a nucleation burst are often drawn according to visual analysis of empirical diagrams of the particle size distribution. The graphical method is successful when the growth of neutral particles larger than about 5 nm is considered. Smaller particles are effectively absorbed by the pre-existing background aerosol particles (Kerminen and Kulmala, 2002) shaping the evolution and complicating the interpretation of measurements. Additional difficulties arise when some amount of particles is born on gaseous ions, thus carrying an inherent electrical charge. The combination and electrical recharging of very small particles are quicker than the growth, and the size distribution can be affected by the electrical processes. The role of ions in the particle generation and evolution is a subject of heated discussions, because the air ionization depends on the extraterrestrial processes and may be a mediator of extraterrestrial factors in the Earth's climate (Svensmark, 1998; Harrison and Carslaw, 2003). Thus the analysis of the electrical properties of fresh aerosol is a topical problem today. If particles smaller than 5 nm are measured and the electrical processes are considered, the simple graphical methods of data analysis appear to be insufficient.

An alternative to the graphical analysis of size distribution diagrams is the numerical simulation of aerosol evolution and fitting simulated distributions to the data. A large number of aerosol evolution models are developed for solving different tasks. Several previous studies expect concentrated sources of particles and nucleating gases like chimneys or roads. They consider aerosol evolution together with spatial dispersion and dilution. A model by Jacobson and Seinfeld (2004) is a good example of a model of this kind. The task of the present study is different. New particles can be expected to be created and homogeneously distributed in space when discussing an atmospheric nucleation burst. Thus the spatial dispersion problems can be omitted. An overview and comparison of models for the simulation of atmospheric nucleation is given by Korhonen et al. (2003). A specific subject of discussions is the role of ions and electrical processes in atmospheric nucleation. Two well known models, which consider

electrical processes, are the models by Yu and Turco (2001) and Laakso et al. (2002). These models include detailed submodels of different processes and their aim is to check the effect of theoretical assumptions regarding the physical and chemical mechanisms of nucleation and particle growth, including the effect of ions and particle charging. These models require considerable computation time for every simulation and are not well adapted for data analysis. The aim of the present simulation model is data fitting that requires a large number of test simulations for every measurement. The necessary computational efficiency can be achieved only when using parametrized submodels for the processes considered in the model. Thus one of the methods in the development of the simulation tool is the computationally efficient parametrization of considered processes. The achieved computational efficiency allows using thousands of sections in a sectional computation model, and the following suppressing of the effect of numerical diffusion. The parameters are considered as external controls in the present model. They can be adjusted during step by step fitting of the data considering simultaneously the physical knowledge and the deviation of the simulated burst from the measurements. The parameters are controlled by the user of the simulation program without the need to modify and recompile the code as in the model by Prakash et al. (2003).

General conventions, presumptions, and simplifications

Particles in the air are classified as molecules, van-der-Waals clusters, macroscopic particles, and ions. Generally speaking all charged particles that play the role of carriers of electric current can be considered as the ions (Loeb, 1955). In the present paper the term "ion" is used to denote the small ions only, whereas charged macroscopic particles that play a role in atmospheric electricity as the intermediate and large ions are not called ions. The small ions are typically charged clusters with electric mobilities of $1\text{--}2\text{ cm}^2\text{V}^{-1}\text{s}^{-1}$ and size of $0.6\text{--}1\text{ nm}$. All small ions of one polarity are expected to be of equal size and mobility, but the parameters of ions of different polarities are considered different.

The term "particle" is used when speaking of macroscopic particles. Clusters and particles are distinguished according to their electron structure and the separation of internal energy levels (see Petrov, 1986). The diameter where the separation of energy levels matches the average thermal energy, is estimated to be about 1.6 nm when fitting the measured mobilities of ions (Tammet, 1995).

The size of a nanoparticle is a conventional model parameter and a subject of different definitions. The size is measured as an effective diameter of a particle. The present model accepts the presumption that the density of the particulate matter ρ is independent of the particle size. The density is included into the list of the control parameters of the model. The particle volume is determined by the mass as $V = m/\rho$. The mass is a well defined quantity and the definition of the particle diameter according to the mass

$$d = \sqrt[3]{\frac{6m}{\pi\rho}} \quad (1)$$

makes it easy to calculate the aerosol mass concentration according to the number concentration and vice versa. The widely used concept of mobility diameter is rejected because the calculation of the mobility diameter assumes a known size-mobility relation but the size-mobility relation can be recognized only when the size is defined independent of the mobility.

Particles are classified into fresh nucleation mode particles born during a nucleation burst, and pre-existing background aerosol particles. The fresh particles are expected to grow in the nanometer and ultrafine size range and the background aerosol particles are expected to be bigger than the largest fresh particles.

The genesis of ions is described by the ionization rate I that depends predominantly on the content of radon and aerosol-carried radon progeny in the air. The sink of ions considers mutual recombination, conversion of the ions to particles, adsorption by the fresh aerosol

particles, and adsorption by the background aerosol particles. The effect of the atmospheric electric field is neglected. This simplification may render the model inadequate when applied to measurements in a strong electric field. In a specific case of measurements like inside the forest canopy, the dry deposition may become an essential factor of ion and nanoparticle evolution. However, this factor is not considered in the present paper.

It is expected that the new particles appear in the air with a fixed initial size that is considered as a model control parameter and usually estimated to be between 1 and 2 nm. The intensity of fresh particle generation is called the nucleation rate and is defined separately for the neutral, positive and negative particles. The mechanism of nucleation is not discussed. The fresh particles are very small and it is assumed that they never carry multiple charges. The evolution of fresh particles is modeled as growth, recharging with encountered ions, and depletion on the pre-existing aerosol particles. The mutual coagulation of fresh particles is neglected with an aim to support the computational efficiency of the algorithms. The last simplification may limit the applications with weak and moderate bursts of nucleation.

Traditionally, the growth of particles is considered by condensation of vapor molecules size of which is neglected. This approach becomes problematic (compare e.g. Hwang et al., 2000), when the added substance consists of large organic molecules or van der Waals clusters. Thus the units of added substance are called "growth units" from here on. This term is adopted from the physics of the crystal growth. The size of the growth units is not neglected and the process of growth is described as the coagulation of particles with growth units. Two kinds of growth units are considered in the model: the first kind is responsible for nucleation and slow initial growth of particles; evaporation of the substance of the first kind of the growth units is neglected. The substance of the second kind of the growth units may evaporate and they are responsible for quicker growth after the particles have passed the threshold size of the nano-Köhler model (Kulmala et al., 2004a).

The coagulation of particles at large Knudsen numbers has been a subject of careful theoretical studies, e.g. by Huang et al. (1990). However, the application of fundamental theory in comparison of simulated and measured processes encounters difficulties because of the shortage of information about the control parameters of sophisticated models. The measurements of nucleation bursts are not of high precision and may consist of indeterminacy up to 10% and even more. In the interpretation of the measurements, simplicity and transparency appear more essential than the exactness of the theoretical model.

Approximations serve the transparency and computational efficiency of the simulator. In the present model, the coagulation of particles and growth units is described using the Sahní interpolation (Fuchs and Sutugin, 1971) between the free molecule and continuum regimes. The attachment of ions to particles is considered according to an approximation of the numerical results by Hoppel and Frick (1986) and measurements by Reischl et al. (1996). Interaction with the induced dipole moments of growth units is included according to the (8–4) potential model (Tammet, 1995). Two alternative methods of accounting for the interaction of charged particles with polar molecules such as sulfuric acid are considered. The first method uses the concept of total effective polarizability and the second method uses the results by Nadykto and Yu (2003). The growth of particles caused by sticking of the evaporating substance is calculated according to a mathematical approximation of the nano-Köhler model (Kulmala et al., 2004a). The ion and particle size-mobility relation is calculated according to the model by Tammet (1995). The effect of van der Waals forces is parametrized using a simplest model, where the parameter is the capture distance between geometric surfaces of the particle and the growth unit.

The initial situation before the nucleation burst is described by user-controlled constants and functions. Some predetermined constants are: temperature, air pressure, mobilities of positive and negative ions, mutual recombination coefficient of ions α , density of ionic matter, density of growth units and particulate matter, diameters of growth units, threshold of the nano-Köhler growth, capture distance of the van der Waals force, polarizabilities or effective

polarizabilities of growth units, values of Nadykto-Yu enhancement factor at two fixed sizes, critical size and extra temperature of quantum retardation of sticking, relations of positive and negative nucleation rates to the neutral nucleation rate. The predetermined functions describe the time variation of ionization rate, the nucleation rate of neutral particles, the concentration and average diameter of pre-existing aerosol particles, and the plain Knudsen growth rates, which are defined as the limiting growth rates for sticky neutral sizeless growth units. The controls of the model are presented in a control file which can be edited using any plain text editor. Additionally, the control file allows to specify the output of the simulator.

Evolution of ions

Equations of evolution and balance of ions

The source of ions is the ionizing radiation measured by the ionization rate I . The sinks of ions are the mutual recombination, the ion-induced nucleation, and the attachment to aerosol particles. The equations of the evolution of the positive and negative ion concentrations n^+ and n^- are

$$\left. \begin{aligned} \frac{dn^+}{dt} &= I - J^+ - \alpha n^+ n^- - (s_n^+ + s_b^+) n^+ \\ \frac{dn^-}{dt} &= I - J^- - \alpha n^+ n^- - (s_n^- + s_b^-) n^- \end{aligned} \right\}. \quad (2)$$

J^+ and J^- are the rates of ion-induced nucleation, α is the recombination coefficient, s_n is the sink of ions on the nucleation mode aerosol, and s_b is the sink of ions on the background aerosol. The sink of ions on aerosol is calculated as an integral over the particle size distribution and divided into two components s_n and s_b because the nucleation mode particles and the background aerosol particles are separately considered in the model. The sinks are discussed in the following sections of the paper. In a steady-state situation the derivatives are of zero value and Equations (2) may be solved to obtain the steady-state concentrations of ions. An algebraic solution is not possible, because the aerosol sinks s_n and s_b depend on the concentrations of ions.

Attachment of ions to neutral and charged particles

The flux of ions dn/dt to large spherical particles is described by the attachment coefficient or the combination coefficient β that is a specific instance of the coagulation kernel or the coagulation coefficient in the ion-particle problem $dn/dt = -\beta n N$ where n is the concentration of ions and N is the concentration of particles.

The attachment of single charged positive ions to a particle with the electric charge qe and diameter d in the continuum regime is described by the Fuchs continuum regime model (Fuchs, 1964)

$$\left. \begin{aligned} x &= 2q \frac{d_q}{d} \\ \beta_q(d) &= 2\pi D d \frac{x}{e^x - 1} \end{aligned} \right\}, \quad (3)$$

where the term $2\pi D d$ is inherited from the Maxwell solution of diffusion equation in a spherically symmetric problem. D is the diffusion coefficient of ions related to the mechanic mobility B and the electric mobility $Z = eB$ of the ions according to Einstein equation

$$D = kTB \approx 8.616 \times 10^{-8} (T : \text{K}) (Z : \text{cm}^2 \text{V}^{-1} \text{s}^{-1}) \text{m}^2 \text{s}^{-1}. \quad (4)$$

The charge index q and the value of x are considered positive for the positive particles and negative for the negative particles. The abbreviation d_q denotes the characteristic length of the Coulomb attachment

$$d_q = \frac{e^2}{4\pi\epsilon_0 kT} \approx 1.671 \times 10^4 / (T : \text{K}) \text{ nm}. \quad (5)$$

Equation (3) overestimates the attachment of the ions to the small particles. Unfortunately, there is no simple and exact theory of the ion attachment for the free molecule regime. Fuchs (1963) developed a limiting sphere model to cover the range of small and intermediate particles. Improvements of the Fuchs model considering the three body trapping of the ions require careful numerical calculations; see Hoppel and Frick (1986).

Troublesome physical calculations are not welcome in a data analysis model that must be computing-efficient. It is reasonable to replace here the physical equations with a formal mathematical approximation of the available tabulated results of measurements and theoretical calculations. The two checkpoints of an approximate model are the converging of model values to the experimental value of the ion-ion recombination coefficient (about $1.6 \times 10^{-6} \text{ cm}^3 \text{ s}^{-1}$) and the fitting of the measurements of nanoparticle charges (e.g. Reischl et al., 1996). A mathematical approximation proposed by Tammet (1991) uses the continuum regime equation (3) with a correction factor

$$1 - \frac{2}{2 + q(q-1) + d/10 \text{ nm}}. \quad (6)$$

Comparison of the approximation with the measurements of charging probability by Reishl et al. (1996) showed that the factor (6) overcompensates the error of the continuum regime equation. In some latter papers (e.g. Tammet et al., 2001) the expression (6) was replaced by the square root of the same expression. However, this results in a small undercompensation.

The model above, as well as the physical model by Hoppel and Frick do not converge to the same value of the ion-ion recombination coefficient when estimating the attachment of negative ions to positive ones and vice versa. The symmetry of ion-ion recombination can be achieved replacing the particle diameter with the sum of the particle and ion diameters $d = d_p + d_i$ and the diffusion coefficient of ions with the mutual diffusion coefficient. The last replacement is problematic, because the effect of the particle diffusion is important only in case of very small particles and high Knudsen numbers where rather the squares of velocities are the subjects to be combined. Thus the term $\sqrt{D_p^2 + D_i^2}$ is used below as a formal mathematical approximation of the joint diffusion factor where D_p and D_i are the diffusion coefficients of particles and ions. Additionally, the effect of van der Waals interaction can be included in the first approximation by adding an extra distance h to the collision distance. The value of the extra distance was estimated $h = 0.115 \text{ nm}$ (Tammet, 1995). When the ion size is taken into account, the correction factor (6) should be modified. A new correction factor is the result of a formal approximation of the data tabulated by Hoppel and Frick (1986) and the diagram by Reischl et al. (1996). The composite model of attachment coefficients for the simulator of bursts of nanoparticles is

$$\left. \begin{aligned} d &= d_p + d_i + 2h \\ x &= 2q \frac{d_q}{d} \\ y &= 1 - \frac{1}{1 + 0.3q(q-1) + d/15 \text{ nm}} \\ \beta_q(d) &= 2\pi dy \sqrt{D_p^2 + D_i^2} \frac{x}{e^x - 1} \end{aligned} \right\}. \quad (7)$$

Some values for positive ions (diameter 0.8 nm and mobility $1.36 \text{ cm}^2 \text{ V}^{-1} \text{ s}^{-1}$) and negative ions (diameter 0.7 nm and mobility $1.56 \text{ cm}^2 \text{ V}^{-1} \text{ s}^{-1}$) calculated according to algorithm (6) are presented in Tables 1 and 2.

Table 1

Attachment coefficients ($10^{-12} \text{ m}^3 \text{ s}^{-1}$) calculated according to algorithm (7) for positive ions, $T = 273 \text{ K}$, $p = 1013 \text{ nm}$, parameters of ion: $d = 0.8 \text{ nm}$, $\rho = 2.08 \text{ g cm}^{-3}$, $Z = 1.35 \text{ cm}^2 \text{ V}^{-1} \text{ s}^{-1}$

$d : \text{nm}$	$q = -3$	$q = -2$	$q = -1$	$q = 0$	$q = +1$	$q = +2$	$q = +3$
0.7	7.98	4.67	1.56	0.0057	0.0000	0.0000	0.0000
1.0	7.09	4.00	1.30	0.0061	0.0000	0.0000	0.0000
1.6	6.13	3.44	1.13	0.0083	0.0000	0.0000	0.0000
2.0	5.94	3.34	1.11	0.0104	0.0000	0.0000	0.0000
3.0	5.85	3.31	1.14	0.0171	0.0000	0.0000	0.0000
5.0	5.86	3.36	1.22	0.0345	0.0000	0.0000	0.0000
10	5.94	3.50	1.39	0.0931	0.0000	0.0000	0.0000
20	6.09	3.71	1.63	0.2444	0.0042	0.0000	0.0000
50	6.40	4.12	2.15	0.7853	0.1882	0.0324	0.0046
100	6.85	4.79	3.05	1.7516	0.8996	0.4172	0.1774
200	8.23	6.50	4.99	3.7249	2.7052	1.9117	1.3159
500	13.7	12.3	10.9	9.6864	8.5512	7.5155	6.5760
1000	23.5	22.2	20.9	19.638	18.461	17.336	16.261

Table 2

Attachment coefficients ($10^{-12} \text{ m}^3 \text{ s}^{-1}$) calculated according to algorithm (7) for negative ions, $T = 273 \text{ K}$, $p = 1013 \text{ nm}$, parameters of ion: $d = 0.7 \text{ nm}$, $\rho = 2.08 \text{ g cm}^{-3}$, $Z = 1.56 \text{ cm}^2 \text{ V}^{-1} \text{ s}^{-1}$

$d : \text{nm}$	$q = +3$	$q = +2$	$q = +1$	$q = 0$	$q = -1$	$q = -2$	$q = -3$
0.8	8.37	4.78	1.56	0.0056	0.0000	0.0000	0.0000
1.0	7.86	4.42	1.43	0.0061	0.0000	0.0000	0.0000
1.6	7.01	3.92	1.29	0.0088	0.0000	0.0000	0.0000
2.0	6.84	3.84	1.28	0.0113	0.0000	0.0000	0.0000
3.0	6.77	3.83	1.31	0.0189	0.0000	0.0000	0.0000
5.0	6.79	3.89	1.41	0.0388	0.0000	0.0000	0.0000
10	6.89	4.05	1.61	0.1064	0.0000	0.0000	0.0000
20	7.06	4.30	1.89	0.2815	0.0048	0.0000	0.0000
50	7.42	4.78	2.48	0.9082	0.2169	0.0372	0.0053
100	7.94	5.55	3.54	2.0285	1.0411	0.4823	0.2049
200	9.54	7.53	5.78	4.3162	3.1341	2.2144	1.5239
500	15.9	14.2	12.7	11.228	9.9116	8.7110	7.6217
1000	27.2	25.7	24.2	22.765	21.401	20.097	18.851

Depletion of ions on nucleation mode aerosol particles

Fresh particles are of nanometer or ultrafine size and can be considered as neutral or single charged during a nucleation event. It is enough to indicate their polarity instead of the charge and the size-charge distribution in a sectional model. The particle distribution can be described by three vectors of the section concentrations N_i^+ , N_i^- , and N_i^0 , where the index i counts the size sections. The sinks $s = -(dn/dt)/n$ of positive and negative ions on these particles are

$$\begin{aligned} s_n^+ &= \sum \beta^{+0}(d_i)N_i^0 + \sum \beta^{+-}(d_i)N_i^- \\ s_n^- &= \sum \beta^{-0}(d_i)N_i^0 + \sum \beta^{-+}(d_i)N_i^+ \end{aligned} \quad (8)$$

where the first polarity index near β denotes the ion charge and the second the particle charge.

Depletion of ions on large particles of background aerosol

In a situation without a nucleation burst the number of nanoparticles is very low and it may be neglected when estimating the sink of the ions. The pre-existing particles of the background

aerosol are much bigger than the ions. Thus the size of an ion and the diffusion of the background aerosol particles can be ignored in this special problem. When the background particles are large enough to accept presumption $x \ll 1$ (see Equations 3 and 7) the mathematical first approximation $x/(e^x - 1) \approx 1 - x/2 = 1 - qd_q/d$ can be used. A corresponding rough approximation of the attachment coefficients of an ion with the diffusion coefficient D to a particle with the size d and the charge qe is

$$\beta_q(d) = 2\pi D(d \pm qd_q), \quad (9)$$

where the sign \pm should be replaced with $-$ in case of positive ions and with $+$ in case of negative ions. The sink of positive ions on the monodisperse background aerosol that consists of particles with different charges qe and corresponding concentrations N_q is

$$s_b^+ = \sum \beta_q^+(d) N_q = 2\pi D^+ \sum d_b N_q - 2\pi D^+ d_q \sum q N_q = 2\pi D^+ (d_b N - d_q N_e), \quad (10)$$

where $d_b N = \sum d_b N_q$ is the diameter concentration or the diameter length of particles in a unit volume of the background aerosol. The typical diameter concentrations of the tropospheric aerosol are several hundreds m/m^3 . $N_e = \sum q N_q$ is the numeric concentration of elementary charges carried by the background aerosol where the positive particles are counted with the positive value of q and the negative particles with the negative value of q .

The sink of negative ions is

$$s_b^- = 2\pi D^- (d_b N + d_q N_e). \quad (11)$$

The depletion of ions on the background aerosol was calculated in papers (Salm, 1987; Tammet, 1991) considering the real size distribution of the background aerosol and not using the approximation $x/(e^x - 1) \approx 1 - x/2$, but assuming the equal mobilities of positive and negative ions. The result (Tammet, 1991) was $g = (2.3 \times 10^{-5} \text{ m}^2 \text{ s}^{-1}) d_b N$ for the ions of the mobility of $1.45 \text{ cm}^2 \text{ V}^{-1} \text{ s}^{-1}$ at 290 K. The corresponding value of $2\pi D$ is $2.28 \times 10^{-5} \text{ m}^2 \text{ s}^{-1}$. It follows the various approximations do not make considerable difference in the results for ions of equal mobilities.

The effect of the polydisperse background aerosol depends on the sum of $d_{bi} N_i$ over the size fractions counted by the index i . This sum equals to $d_b N$, where d_b is the average diameter and N is the total concentration of background particles. Hence the polydisperse background aerosol can be replaced in the model by an equivalent monodisperse aerosol with the particle diameter of d_b .

Condensation, coagulation and depletion of particles

Sahni model for condensation in transitional regime

Vapor condensation is a factor of particle growth in the nanometer size range. Another application of the condensation theory is the problem of Brownian coagulation because this process is mathematically similar to the problem of vapor condensation on particles. There exist exact solutions of the simplified condensation problem in the continuum limit and in the free molecule or kinetic limit. The molecules are expected to be of zero size, the particles are considered as sticky hard spheres, and the distant forces are neglected in a simplified problem. The flux of molecules of the concentration n to a particle of the diameter d in the continuum limit is expressed by Maxwell equation

$$\phi_c = 2\pi D d n, \quad (12)$$

and in the free molecule or kinetic limit by Knudsen equation

$$\phi_k = (\pi/4) d^2 u n, \quad (13)$$

where D is the diffusion coefficient and u is the average kinetic velocity of the molecules of mass m :

$$u = \sqrt{\frac{8kT}{\pi m}}. \quad (14)$$

The theory of the transitional regime is complicated and different approximate solutions are known. The limiting sphere model by Fuchs refined by Fuchs and Sutugin (1971) is widely used (e.g. Kulmala et al. 2001). A computationally more efficient alternative is the Sahni model recommended by Fuchs and Sutugin (1971). Formally, the Sahni model is an interpolation between the exact models of continuum regime and free molecule regime. The transitional regime is characterized by the ratio

$$\gamma = \frac{\Phi_c}{\Phi_k}, \quad (15)$$

which is a replacement of the Knudsen number. If the mean free path is defined according to an obsolete tradition as $l_o = 3D/u$ and the Knudsen number as $Kn = 2l_o/d$, then $\gamma = (4/3) Kn$. Usage of the ratio γ instead of the Knudsen number is motivated by the aim to write expressions independent of the concept and definition of the mean free path.

The simplest interpolation formula known as the Sherman universal formula is a harmonic mean $\Phi = 1 / (1/\Phi_c + 1/\Phi_k) = \Phi_c / (1 + \gamma)$ similar to the formula of parallel resistors in electricity. The Sahni's interpolation equation for "black" sphere condensation in transitional regime is written in above terms as

$$\Phi = \frac{\Phi_c}{1 + \kappa\gamma} = \frac{\Phi_k}{\kappa + 1/\gamma}, \quad (16)$$

where κ is a specific function of γ tabulated by Sahni according to complicated numerical calculations. Fuchs and Sutugin presented a table of $\lambda = (4/3)\kappa$ as a function of $Kn^{-1} = (4/3)/\gamma$ together with a mathematical approximation. Unfortunately the error of this approximation exceeds 6%. Thus an improved mathematical approximation is proposed

$$\kappa \approx 1 - \frac{0.299}{\gamma^{1.1} + 0.64}, \quad (17)$$

which deviates from the table presented by Fuchs and Sutugin (1971) less than 0.3%.

Condensation of molecules on a "gray" sphere can be calculated according to Fuchs and Sutugin using a modified Sahni equation

$$\Phi = \frac{\Phi_c}{1 + \left(\kappa + \frac{1-p}{p} \right) \gamma} = \frac{\Phi_k}{\kappa + \frac{1}{\gamma} + \frac{1-p}{p}} \quad (18)$$

where p is the sticking probability.

Effects of the size of growth units and the attractive van der Waals force

If the attaching growth units are large molecules or clusters, the assumption of the zero size turns out inadequate and a growth unit is to be considered as a second particle (see also Lehtinen and Kulmala, 2003). Different from the calculations above, the sizes of both particles are to be taken into account, the radius of the particle is to be replaced with the collision distance δ , and the diameter with the double collision distance. The collision distance is defined from the equation $\Omega = \pi\delta^2$, where Ω is the collision integral (Chapman and Cowling, 1970) that equals to the particle cross section in the model of the collision of a sizeless molecule with a hard sphere. The collision distance is the sum of the radii of the colliding particles in a plain geometric model of two hard spheres. An attempt to approximate the measured mobilities of ions using the (8-4) potential model showed that the measurements can be well fitted when the effective collision distance is expected to be a little bigger than the sum of radii (Tammet, 1995), which compensates the disregarding of the van

der Waals force in the plain geometric model. The theory of the effect of van der Waals force on nanoparticle coagulation is complicated (see e.g. Alam, 1987) and its application may encounter difficulties due to the lack of information about the Hamaker constant. The interparticle van der Waals force decreases rapidly with increase in the distance between the surfaces of the interacting particles (Nelson, 1995). When the closest distance of free flight approach is less than the distance where the van der Waals potential exceeds the thermal kinetic energy, the particles may be coagulated. This allows to introduce an extra capture distance between the particle surfaces h as a parameter of the simplest empirical model. The extra distance should be added to the geometric collision distance when expressing the effective interception of particles. In the present model the effect of the van der Waals force is included into the interception enhancement factor of the growth rate and the collision distance is calculated as

$$\delta = d_1/2 + d_2/2 + h, \quad (19)$$

where d_1 and d_2 are the geometric diameters of the colliding particles. The value of the extra addend was estimated $h = 0.115$ nm when approximating the empirical particle size-mobility relation (Tammet, 1995), but it can be different in a problem of two particles depending on the value of the Hamaker constant. Thus the extra distance is considered as an empiric control parameter of the model and its value may be estimated fitting the measurements.

Brownian coagulation of neutral particles

In kinetic calculations, the particles are treated as large molecules and the coagulation of particles is considered as a condensation of one kind of particles on the particles of the other kind. The flux of neutral particles of size d_1 and concentration N_1 to neutral particles of size d_2 and concentration of N_2 in a volume unit is expressed as

$$\phi = K_o(d_1, d_2)N_1N_2, \quad (20)$$

where K_o is the coagulation coefficient or coagulation kernel for two neutral particles.

When translating the condensation equations, the diffusion coefficient is to be replaced with the mutual diffusion coefficient of particles $D_1 + D_2$, the radius of the particle with the collision distance δ , and the average velocity with the average relative velocity. The translated equations are:

$$\text{Maxwell equation} \quad K_c = 2\pi(D_1 + D_2)(d_1 + d_2 + 2h), \quad (21)$$

$$\text{Knudsen equation} \quad K_k = (\pi/4)(d_1 + d_2 + 2h)^2 u_{12}, \quad (22)$$

$$\text{average relative velocity} \quad u_{12} = \sqrt{\frac{8kT(m_1 + m_2)}{\pi m_1 m_2}}, \quad (23)$$

where m_1 and m_2 are masses of particles,

$$\text{the ratio} \quad \gamma = \frac{K_c}{K_k}, \quad (24)$$

$$\text{and the Sahni's interpolation} \quad K_o = \frac{K_c}{1 + \kappa\gamma}. \quad (25)$$

The composite algorithm for the calculation of the coagulation coefficient of two neutral particles is written as follows:

$$\left. \begin{aligned} \gamma &= 2 \frac{B_1 + B_2}{d_1 + d_2 + 2h} \sqrt{\frac{2\pi k T m_1 m_2}{m_1 + m_2}} \\ K_o &= \frac{2\pi k T (B_1 + B_2)(d_1 + d_2 + 2h)}{1 + \gamma - \frac{0.299\gamma}{\gamma^{1.1} + 0.64} + \gamma \frac{1-p}{p}} \end{aligned} \right\}, \quad (26)$$

where B_1 and B_2 are the mechanic mobilities of particles.

Effect of electric charge in case of non-polar growth units

The electric field of a charged particle E induces a dipole moment αE of a growth unit independent of its permanent polarization, the constant α is called the polarizability. The induced dipole moment has a definite orientation and the average force in the converging electric field of a charged particle is not zero. The charge-induced dipole interaction results in an enhanced cross-section of a collision between a particle and a molecule. The effect of higher polarization moments is low and not considered in the present model.

A simple tool for estimating the enhancement of the collision cross section by the induced dipole interaction is the $(\infty-4)$ potential model well known in the kinetic theory of ion mobility (McDaniel and Mason, 1973; Mason and McDaniel, 1988). The model of $(\infty-4)$ interaction potential

$$U = \begin{cases} \text{if } r < \delta & \text{then } \infty \\ \text{if } r > \delta & \text{then } U_{\text{pol}}(r) \end{cases} \quad (27)$$

combines the hard sphere repulsion and the polarization attraction. r is the distance between the point charge located in the center of the particle and the center of the encountering growth unit. In the limit $U_{\text{pol}} = 0$ the model reduces to the hard sphere model for neutral particles just as considered above. The potential of polarization interaction is

$$U_{\text{pol}}(r) = -\frac{\alpha e^2}{8\pi\epsilon_0 r^4}, \quad (28)$$

where e is the particle charge and α is the dipole polarizability of a growth unit. The equation above is written according to tradition so that α is to be measured in m^3 like in the electrostatic system of units but other quantities are expressed in SI. Polarizability of a conductive sphere is R^3 , where R is the radius of the sphere. Polarizability of molecules expressed in \AA^3 can often be roughly estimated as equal to the number of atoms in the molecule.

The collision integral for the $(\infty-4)$ potential can be calculated numerically. The electric factor of the coagulation coefficient is expressed with the dimensionless collision integral Ω^* , which is the ratio of the $(\infty-4)$ collision integral Ω to the hard sphere collision integral

$$\Omega^* = \Omega / (\pi\delta^2) \quad (29)$$

and the coagulation coefficient is to be calculated as

$$K = \Omega^* K_0, \quad (30)$$

where K_0 is the coagulation coefficient for two neutral particles (Equation 26).

The integral Ω^* is tabulated according to the results of numerical calculations as a function of temperature (see McDaniel and Mason, 1973). Traditionally, the dimensionless temperature $T^* = |kT/U_{\text{pol}}(\delta)|$ is considered as the argument. The table can be replaced by an approximation (Tammet, 1995):

$$\Omega^* = \begin{cases} \text{if } T^* \leq 1 & \text{then } 1.4691 \times T^{*-1/2} - 0.341 \times T^{*-1/4} + 0.182 \times T^{*5/4} + 0.059 \\ \text{if } T^* \geq 1 & \text{then } 1 + 0.106 \times T^{*-1} + 0.263 \times T^{*-4/3} \end{cases} \quad (31)$$

The approximation is correct in the limit $T^* \rightarrow 0$ and the relative error of the calculated values is less than 0.1%, when compared with the table calculated in the first approximation of the Chapman-Enskog method and published in the book by McDaniel and Mason (1973).

The integral Ω^* can be interpreted as the enhancement coefficient of the growth of charged particles coagulating with the non-polar growth units. The value of this coefficient exceeds the value of 1 typically only for a few percent and approaches quickly to 1 when the particle

size is increasing. This conclusion does not agree with a proposition by Yu and Turco (2001), who compared the attachment coefficients for ions and neutral molecules when encountering a nanoparticle and found the ratio to be about ten. They presented the graph of the ion-particle attachment coefficient with the explanation "one charged and one neutral particle" and probably used the same value of the attachment coefficient when calculating the condensation of neutral molecules on charged particles. However, the coagulation rate for a large charged particle and a neutral molecule or cluster is much less than the coagulation rate for a large neutral particle and a small ion. The reason is that the induced dipole moment increases rapidly with the volume of the neutral particle and the electric field on the surface of a small charged particle is stronger than on the surface of a large charged particle. This makes a big difference between the two variants of the problem "one charged and one neutral particle".

Effect of electric charge in case of polar growth units

Growth units, e.g., molecules of sulfuric acid, may have a permanent dipole moment. Permanent dipoles have a random orientation and when the distribution of the orientations is not disturbed, then the average electric force is zero (McDaniel and Mason, 1973). The electric field of a charged particle disturbs the distribution of permanent dipole orientations that creates some attracting force. The effect is similar to the effect of an induced dipole moment and the two effects may be added. In this case the polarizability is to be replaced by the total effective polarizability (see Loeb, 1955). The effective polarizability is calculated as follows (see Nelson et al., 2001):

$$\alpha_{eff} = \alpha + \frac{\mu^2}{6\pi\epsilon_0 kT}, \quad (32)$$

where μ is the permanent dipole moment of a growth unit. As an exception, Equation (32) is written in the specific system of units where polarizability is measured in m^3 and all other quantities in SI like in Equation (28). The effective polarizability can essentially exceed the standard dipole polarizability. Example: a molecule of sulfuric acid has a dipole polarizability $\alpha = 6.2 \text{ \AA}^3$ and a permanent dipole moment $\mu = 2.84 \text{ Debye} = 9.47 \times 10^{-30} \text{ C m}$. A calculation according to Equation (32) at $T = 273 \text{ K}$ results in $\alpha_{eff} = 149 \text{ \AA}^3$ that exceeds the dipole polarizability about 24 times.

Nadykto and Yu (2003) proposed an independent theoretical estimate of the effect of dipole moment on the coagulation coefficient and found a large enhancement factor En up to the values of about five in case of 1 nm particles. They presented diagrams of the function $En(d)$ for different polar molecules including water, sulfuric acid, and ammonia. The enhancement of growth according to Nadykto and Yu (2003) is much less than that according to Yu and Turco (2001). In the present model the enhancement factor of Nadykto and Yu is parametrized using an exponential approximation where the parameters are the reference values of the enhancement factor at two values of diameter 1 nm and 2 nm:

$$\left. \begin{aligned} a &= (En(1 \text{ nm}) - 1)^2 / (En(2 \text{ nm}) - 1) \\ b &= \ln((En(1 \text{ nm}) - 1) / (En(2 \text{ nm}) - 1)) \\ En(d) &= 1 + a \exp(-bd) \end{aligned} \right\}, \quad (33)$$

where d should be expressed by its numerical value in nanometers. According to Nadykto and Yu (2003), the reference values for sulfuric acid are $En(1 \text{ nm}) = 4.35$ and $En(2 \text{ nm}) = 1.8$ at temperature 298 K.

The method of the total effective polarizability and the Nadykto-Yu enhancement factor should not be used simultaneously. If the polarizability is presented as the total effective polarizability then the Nadykto-Yu reference values should be evaluated as 1 in the set of the control parameters of the model.

Depletion of nanoparticles

Nanoparticles are depleted by absorption on large particles of the pre-existing background aerosol. The sink of nanoparticles on the pre-existing large particles is to be calculated according to the transitional regime model. The sink of particles of size d_1 is expressed as integral

$$S_b(d_1) = -\frac{1}{N_1} \frac{dN_1}{dt} = \int K(d_1, d_2) \frac{dN}{dd_2} dd_2, \quad (34)$$

where K is the coagulation coefficient and dN/dd_2 is the size distribution of the background aerosol particles. In the first approximation the background aerosol is represented by the monodisperse particles of average diameter of the actual aerosol d_b and the concentration N . This follows the estimate of the sink of nanoparticles of diameter d_1

$$S_b(d_1) = K(d_1, d_b)N, \quad (35)$$

Growth of particles

Growth rate and the plain Knudsen model

In the present paper, the kinetic approach to the growth problem is used. Evaporation-free growth of a particle is considered as sticking of units of additional substance to the particle and following sintering of the aggregate. The growth units may be small molecules, large organic molecules or the van der Waals clusters of molecules. The size of a growth unit may be comparable with the size of a small growing particle. Thus the coagulation equations (26, 30) are a suitable model of the collecting of growth units by a particle. The role of ions as the growth units is expected to be negligible, but the charge of growing particle is a subject to be considered.

The particle diameter growth rate in the free molecule regime is

$$G = \frac{2\phi V_g}{\pi d_p^2} = \frac{\phi d_g^3}{3d_p^2} = \frac{K(d_g, d_p) d_g^3 n_g}{3d_p^2}, \quad (36)$$

where ϕ is the number flux of growth units, d_p is the diameter of particle, V_g , d_g , and n_g are the volume, diameter and concentration of growth units.

A plain Knudsen model is the limit of simplification: the Knudsen equation (13) is accepted, the particles are assumed to be absolutely sticky, the size of growth units and the diffusion of particles are neglected. In this model the square of particle size is cancelled out in Equation (36) and the plain Knudsen growth rate G_o does not depend on the particle size:

$$G_o = \frac{\pi}{12} d_g^3 n_g \sqrt{\frac{8kT}{\pi m_g}}. \quad (37)$$

It is difficult to obtain immediate information about the concentration of growth units in the air. The concentration is often estimated on the basis of the measured growth rate. Thus the plain Knudsen growth rate is a proper empirical parameter of the model and the growth rate is expressed as

$$G = 2 \frac{K(d_g, d_p)}{d_p^2} \sqrt{\frac{m_g}{2\pi kT}} G_o, \quad (38)$$

where the coagulation coefficient K can be calculated according to Equations (26, 30, 31).

Effect of quantum rebound

The coagulation coefficient depends on the sticking probability at the encounter of the growth unit and the particle. If the particles are of the size of about 3 nm and more, the sticking probability is expected to be $p = 1$ (Kulmala et al., 2001). The physics of the capture of

molecules by a surface is analyzed by Clement et al. (1996), expecting that the surface is of a large particle. The sticking probability may decrease when the particles are very small. If the both encountering particles are of a molecular size, then the collisions turn up to be elastic and the sticking probability is $p = 0$ as a rule. Exceptions are the collisions between the molecules of high binding energy. A physical reason for the elastic character of ordinary binary collisions of molecules is kinetic energy conservation in a situation where the colliding particles are not able to absorb energy inside. This is a result of quantum effect: if the collision energy is less than the separation of the internal energy levels of particles, the internal energy of particles remains "frozen". When atoms are assembled in a solid body, then every atom adds its electron levels but the width of the band of energy levels stays about the same. Thus the average spacing of energy levels decreases with increase in the particle mass. Typical kinetic energy of thermal motion is about 0.02 eV. If the spacing of particle internal energy levels will be about the energy of thermal motion or less, then they can be excited, kinetic energy can be absorbed and the colliding growth unit can be affixed to the particle. The process of transfer is called "melting of internal degrees of freedom". In simple models the energy levels of the clusters are expected to be equally spaced (see e.g. Lovejoy et al., 2001). Einstein (1914) explained the temperature dependence of heat capacity by a factor of $(\Delta E / kT)^2 e^{\Delta E / kT} / (e^{\Delta E / kT} - 1)^2$ where ΔE is the spacing of energy levels. The cluster ion empirical mobilities were successfully fitted expecting that the melting of internal degrees of freedom follows the Einstein law (Tammet, 1995). The average spacing of internal energy levels in a nanoparticle or a cluster is in the first approximation inversely proportional to the number of the atoms in the particle or cluster (Petrov, 1986) or to the value of d^3 . Thus the effect of quantum rebound can be approximately described by the model that has two degrees of freedom expressed by two empiric parameters T_o and d_o :

$$p = \frac{x^2 e^x}{(e^x - 1)^2}, \quad (39)$$

where

$$x = \frac{273\text{K}}{T + T_o} \left(\frac{d_o}{d} \right)^3. \quad (40)$$

The effect of the chemical binding energy discharged at the collision is expressed by the extra temperature T_o in Equation (40). Critical diameter d_o can be interpreted as the diameter of a particle in which the average spacing of energy levels is about the same as the energy $k(T + T_o)$ at temperature 273 K. The values of parameters should be estimated fitting the measurements. An estimate $d_o = 2.48$ nm at $T_o = 0$ was found fitting the measured mobilities of ions (Tammet, 1995). This estimate could be used as a reference point when only the kinetic energy is discharged at a collision.

The model (39, 40) does not consider a possible drain of kinetic energy by a third body, which may increase the sticking probability. However, the three-body collisions are rare and have a considerable effect only at very low values of the sticking probability.

Usage of the above model can be hindered by the lack of information about the chemical binding energy. More exact model in the size range below 1.6 nm could be composed using the methods of chemical kinetic, see Luts and Salm (1994).

Discussion of the growth rate factors

The quantitative role of different factors of growth is illustrated in Figure 1. The parameters of the growth units correspond to the parameters of a molecule of sulfuric acid.

The first graph marked as "Plain Knudsen" corresponds to the model that neglects all factors: transition to diffusion regime, mobility of particles, size of growth units, the van der Waals force, quantum rebound and the effect of particle charge. All six graphs are presented relative to the plain Knudsen growth rate, thus all points of the first graph have ordinate 1.

The second graph is marked "Diffusion incl.". Here are included two additional factors. The diffusion of particles accelerates the growth of smallest particles and the transition to the continuum regime decelerates the growth of large particles. The effect is pretty low in the size range that is important when simulating the nucleation bursts.

The third graph is marked "Interception incl.". Additionally, the size of growth units and the van der Waals extra distance are considered, but the quantum rebound and particle charge effect are still neglected. The collision cross section is essentially increased by the size of a growth unit if this size is comparable with the particle size. The molecules of sulfuric acid are large and the effect is strong in the example.

The fourth graph is marked "Quant-rebound incl.". This graph includes all the considered factors for neutral particles. The critical size has a realistic value, but the effect of chemical energy is neglected ($T_0 = 0$). Thus the accommodation of growth units is suppressed up to the size of about 3 nm. Increase in the value of T_0 would be result in decrease in the maximum size where the effect is considerable.

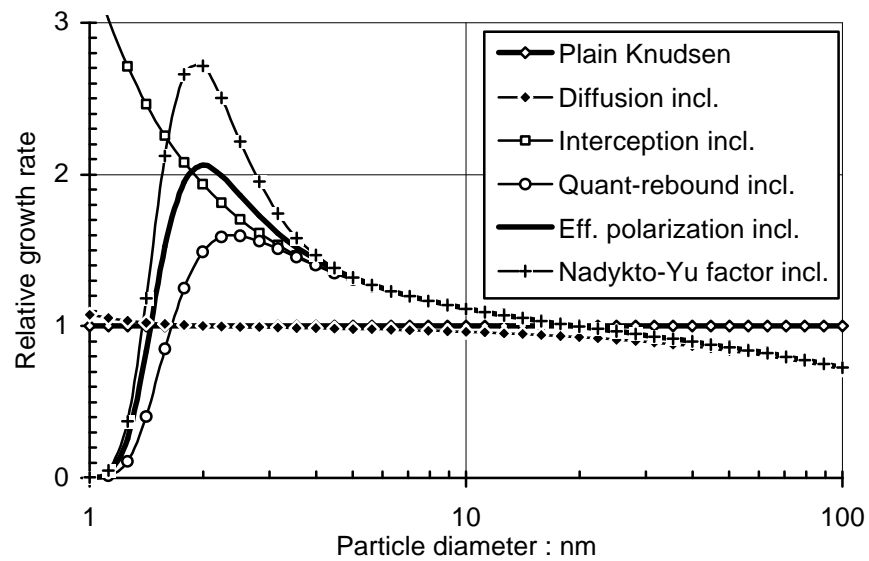


Figure 1. Growth rate calculated at sequential including of factors,
 $d_g = 0.55$ nm, $h = 0.115$ nm, $d_o = 2.5$ nm, $T = 298$ K, $T_0 = 0$,
 $\alpha = 6.2 \text{ \AA}^3$, $\alpha_{eff} = 137 \text{ \AA}^3$, $En(1 \text{ nm}) = 4.35$, $En(2 \text{ nm}) = 1.8$.

The fifth graph marked as "Eff. polarization incl." is calculated for single charged particles using the method of total effective polarizability. The main increase in the growth rate is caused by the permanent dipole moment of the molecules of sulfuric acid. The graph, where only the induced dipole effect is considered, is not presented in the diagram because it would be too close to the graph "Quant-rebound incl.".

The sixth graph marked as "Nadykto-Yu factor incl." includes in addition to the factors considered in "Quant-rebound incl." the Nadykto-Yu enhancement factor. If both methods were exact, then the two last graphs should be merging. However, the difference is considerable. If in a computing experiment the permanent dipole effect in the method of effective polarizability was written twice of the actual value and then the two graphs merged. The controversy is not solved in the present study and the simulation program offers free choice between two alternative methods: the method by Nadykto and Yu or the method of effective polarizability.

Evaporation and the nano-Köhler factor

The condensed substance may evaporate back to the air. In the terms of the kinetic approach this means the thermal detachment of the units of condensed substance. The evaporation

decreases the growth rate and may be described by a factor of growth rate. This factor is defined according to an approximation of the nano-Köhler law (Kulmala et al., 2004a) and called the nano-Köhler factor in the present model. The Köhler law can be written for the growth rate as follows:

$$G = G_o \left(1 - \frac{d_K}{d} + \left(\frac{d_R}{d} \right)^3 \right), \quad (41)$$

where G_o is the growth rate calculated without evaporation, d_K is the Kelvin characteristic size and d_R is the Raoult characteristic size. When decreasing the size, the growth rate turns to zero at the diameter that corresponds to the equilibrium size of the particle. This is the nano-Köhler threshold diameter at which the condensation starts. In the nanometer range, the Köhler law is an approximation and it may be replaced by a mathematical approximation that is more convenient to parametrize and use in fitting of the measurement. In the present model the nano-Köhler law is approximated with a growth rate factor f_{nK}

$$\text{if } d < d_o \text{ then } f_{nK} = 0 \text{ else } f_{nK} = 1 - \left(\frac{d}{d_o} \right)^p, \quad (42)$$

where the nano-Köhler threshold diameter d_o and the power p are the control parameters that should be fitted to the measurement.

Implementation of the simulator

Two condensing substances

The mechanism of nucleation is not considered in the model and the nucleation is described by the nucleation rates for neutral, positive and negative particles. The initial size of particles is considered as a model control parameter. The newly born particles will grow according to the growth models described above. Two kinds of growth units are allowed, the first kind is responsible for nucleation and slow initial growth of particles and the second for quicker growth after passing the threshold size of the nano-Köhler model. If the particle size exceeds the nano-Köhler threshold the two substances are condensing simultaneously.

The first condensing substance is expected not to evaporate. The user-controlled parameters for the first substance are the diameter of growth units, the polarizability or effective polarizability, or the values of Nadykto-Yu enhancement factor at particle sizes of 1 nm and 2 nm, the plain Knudsen growth rate that can be described with a parabolic trend in time, the critical size and the extra temperature of quantum rebound.

The second condensing substance is expected to be able to evaporate. Thus the critical diameter and the power of the nano-Köhler factor (42) are included into the set of the control parameters. The diameter and polarizability of growth units may have different values for two substances. The effect of quantum rebound and the Nadykto-Yu enhancement factor are neglected in case of the second substance, because these effects decrease rapidly with size and the particles with the size below of the nano-Köhler threshold diameter are not subjects to uptake the growth units of second kind.

Outline of the algorithm

The distribution of particles is described in a sectional model by the section concentrations N_i corresponding to diameter sections $(d_{i-1} \dots d_i)$. The growth of particles from i -th section to $(i+1)$ -th section during a short time interval Δt depends on the average values of the particle size distribution function $f(d) = dN/dd$ and the growth rate G around the size d_i during Δt . If the effect of electric charge is neglected the growth can be expressed in the sectional model exactly using the growth-consistent segmentation where $d_{i+1} = d_i + G\Delta t$. The growth-consistent segmentation excludes the effect of numerical diffusion when integrating the

evolution equations. Unfortunately, the effect of electric charge makes the growth-consistent segmentation in the low nanometer size range impossible because a particle may grow with different rates when repeatedly recharged during its evolution. The uniform distribution of sections on linear scale is used in the present model. It follows in a large number of sections that is compensated by good approximation of the growth process and the simple algorithm that supports rapid computation. The width of a section $\Delta d = d_i - d_{i-1}$ is chosen as a minimum width when the replacement of interpolation with extrapolation is excluded: $\Delta d > G_{max}\Delta t$.

Computer experiments including the interpolation approximation of the particle size distribution showed that the integration of the growth may not provide a stable solution because of the amplification of oscillations in the distribution function that happens after rapid changes in the nucleation rate. The stability depends on the interpolation method. Most safe is the simplest algorithm of growth transfer of particles from section to section

$$\Delta N_{i \rightarrow i+1} = \frac{G(d_i)\Delta t}{\Delta d} N_i \quad (43)$$

that assures a stable solution in all situations. The numerical diffusion and computational error are suppressed by increasing the number of sections. The computing efficiency of the simulator remains satisfactory even when the number of sections exceeds 10,000.

The environmental situation and the conditions of the nucleation burst are described in a file of control parameters. Most of environmental parameters can be presented with a parabolic trend. Total number of parameters controlled by the control file is 94. The algorithm includes three main stages.

At first stage the control file is analyzed and the values of the following quantities are calculated and tabulated in memory for the full period under consideration:

- background aerosol average diameter and concentration,
- ionization rate I and nucleation rates J^+ , J^- , J^0 for charged and neutral particles as functions of time,
- growth rates $G_i = G(d_i)$ of particles for all sections (Equations 26, 30, 31, 38),
- attachment coefficients of ion (first polarity index) to particle (second polarity index) β_i^{+0} , β_i^{-0} , β_i^{+-} , β_i^{-+} for all sections (Equation 7),
- particle sinks on background aerosol S_{bi} for all sections (Equations 26 and 35).

The concentrations of the nucleation mode particles N_i in all sections are set to zero and the steady-state concentrations of the ions and the background aerosol charge are calculated according to Equation (2) for the pre-burst situation. Additionally, the initial values of total sinks of particles S_i^+ , S_i^- , and S_i^0 are calculated for all sections.

The second stage is the integration of the evolution equations according to a simple Euler method. A step of evolution consists of one equation of the background aerosol charge evolution, two equations of ion evolution and three equations of particle evolution. The ion sinks on aerosol particles (Equations 8, 10, 11) cannot be calculated in the first stage and they are calculated in every step of the integration process. The simplified algorithm of the step of integration is presented as Equation (44) where $\delta_{1,i}$ is the Kronecker symbol: if $i = 1$ then $\delta_{1,i} = 1$ else $\delta_{1,i} = 0$.

$$\left. \begin{aligned}
\frac{\Delta N_e}{\Delta t} &= s_b^+ n^+ - s_b^- n^- + \sum S_b (N_i^+ - N_i^-), \\
\frac{\Delta n^+}{\Delta t} &= I - J^+ - \alpha n^- n^+ - \left(s_b^+ + \sum \beta_i^{+o} N_i^o + \sum \beta_i^{+-} N_i^- \right) n^+, \\
\frac{\Delta n^-}{\Delta t} &= I - J^- - \alpha n^- n^+ - \left(s_b^- - \sum \beta_i^{-o} N_i^o + \sum \beta_i^{-+} N_i^+ \right) n^-, \\
\frac{\Delta N_i^+}{\Delta t} &= \delta_{1,i} J^+ + (1 - \delta_{1,i}) \frac{\Delta N_{i-1 \rightarrow i}^+}{\Delta t} - \frac{\Delta N_{i \rightarrow i+1}^+}{\Delta t} + \beta_i^{+o} n^+ N_i^o - (\beta_i^{+-} n^- + S_{bi}) N_i^+, \\
\frac{\Delta N_i^-}{\Delta t} &= \delta_{1,i} J^- + (1 - \delta_{1,i}) \frac{\Delta N_{i-1 \rightarrow i}^-}{\Delta t} - \frac{\Delta N_{i \rightarrow i+1}^-}{\Delta t} + \beta_i^{-o} n^- N_i^o - (\beta_i^{-+} n^+ + S_{bi}) N_i^-, \\
\frac{\Delta N_i^o}{\Delta t} &= \delta_{1,i} J^o + (1 - \delta_{1,i}) \frac{\Delta N_{i-1 \rightarrow i}^o}{\Delta t} - \frac{\Delta N_{i \rightarrow i+1}^o}{\Delta t} \\
&\quad + \beta_i^{-+} n^- N_i^+ + \beta_i^{+-} n^+ N_i^- - (\beta_i^{+o} n^+ + \beta_i^{-o} n^- + S_{bi}) N_i^o.
\end{aligned} \right\} \quad (44)$$

In the third stage the export values are calculated using the data collected during the second stage. The list of the export variables may include the ion concentrations, background aerosol charge, average size of neutral and charged nanoparticles in a prescribed size range or in the full size range, index of charge asymmetry of particles, fraction concentrations or values of the size distribution function according to the rules specified in the file of control parameters. The algorithm used in the computer program of the simulator differs from that explained above only in technical details and in some formal transformations that accelerate the calculations.

Example of simulation of a nucleation burst

Figure 2a is built according to the results of simulation in the following conditions: temperature 0°C, pressure 1013 mb, ionization rate $5 \text{ cm}^{-3} \text{ s}^{-1}$, mobilities of positive and negative ions 1.36 and $1.56 \text{ cm}^2 \text{ V}^{-1} \text{ s}^{-1}$, recombination coefficient $1.6 \times 10^{-6} \text{ cm}^3 \text{ s}^{-1}$, density of ions 2.08 g cm^{-3} , birth size of particles 1.5 nm , no ion-induced nucleation, maximum of neutral nucleation rate $10 \text{ cm}^{-3} \text{ s}^{-1}$, size and density of non-evaporating growth units of the first condensing substance 0.55 nm and 2 g cm^{-3} , effective dipole polarizability includes the effect of permanent dipole moment and equals 149 \AA^3 , the plain Knudsen growth rate 1.5 nm/h , critical size and extra temperature of quantum rebound 2.5 nm and 1000 K , size of growth units of second condensing substance 0.8 nm , plain Knudsen growth rate 10 nm/h , the nano-Köhler threshold diameter 3 nm and the power of the nano-Köhler approximation 2 , average diameter and concentration of background aerosol particles 200 nm and 1000 cm^{-3} . The variation of nucleation is described by the relative nucleation rate defined as the ratio of the nucleation rate to its maximum value and multiplied to a scaling factor of 5 for better presentation in Figure.

Figure 2b is built in the same conditions; the only difference is that half of the new particles are expected to be born on negative ions. Thus the maximum of the negative ion-induced nucleation rate and the neutral nucleation rate both equal to $5 \text{ cm}^{-3} \text{ s}^{-1}$. This example shows that the effect of ion-induced nucleation should be visible at first in measurements of ion concentrations.

Calculating of data for one Figures 2a or 2b (3600 time steps by 1.5 s and 2727 size sections between 1.5 and 15.5 nm) with the simulator program takes about 6 seconds on a 1 GHz Pentium processor.

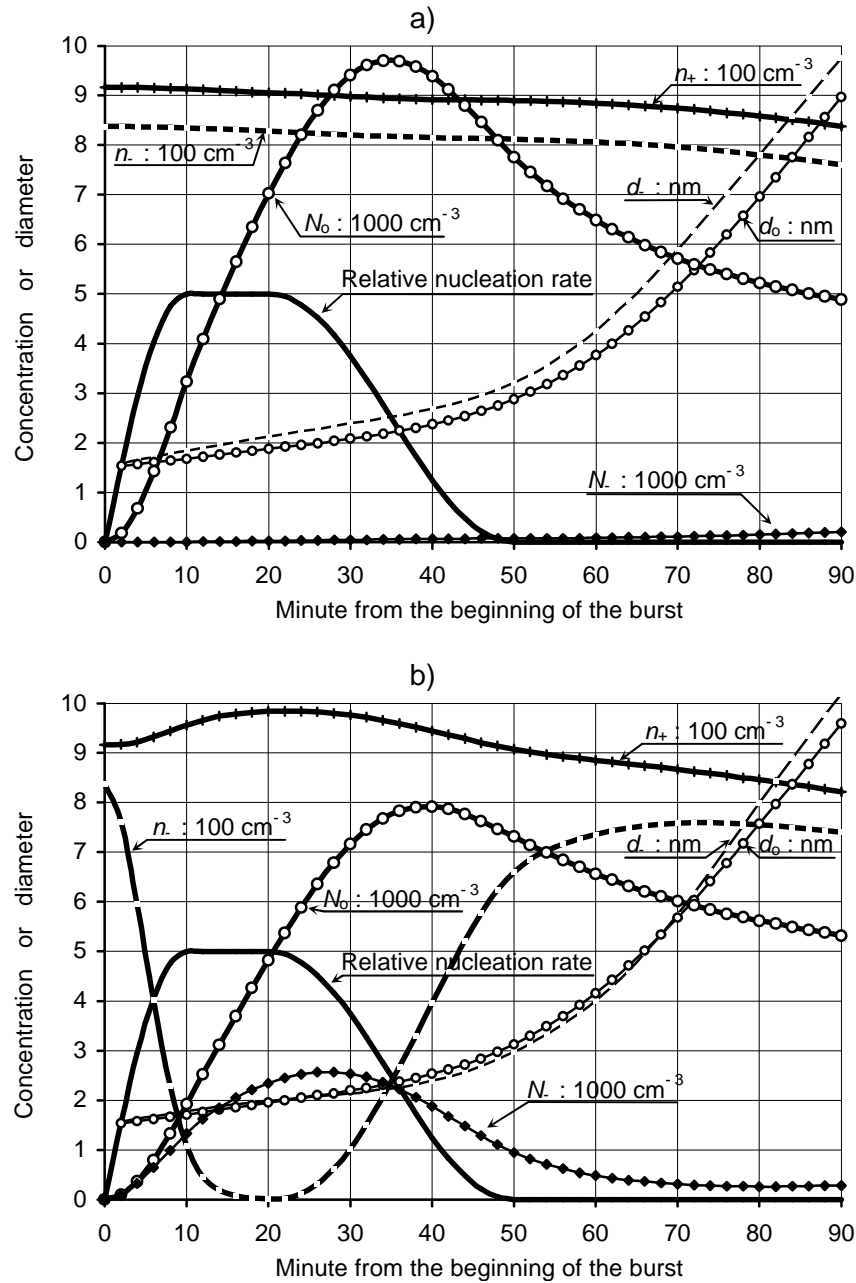


Figure 2. Simulated nucleation burst: a) neutral nucleation, b) combination of neutral and negative ion-induced nucleation. The relative nucleation rate is multiplied by factor of 5. n_+ and n_- are the concentrations of ions, d_- and d_0 are the diameters of negative and neutral particles, N_0 and N_- are the concentrations of fresh neutral and negative particles. Conditions are explained in the text.

Summary

The simulation model described in the present paper has in view the fitting of aerosol and ion measurements for interpretation of the nucleation bursts. Thus the model has a large number of input parameters, which can be adjusted by the user of the simulator when editing the input file. The total number of the user-controlled parameters including the parameters of the structure of the output files is 94. The time variation of the nucleation rate during a simulated nucleation burst can be described with five parameters. The variation of several environmental parameters like the ionization rate, nucleation rates, plain growth rates etc. can be described with a parabolic trend in time. The set of physical assumptions is minimized and the nucleation mechanism is not discussed at all. Instead of this, the nucleation rates for

neutral, positive, and negative particles are considered as control parameters and can be adjusted when fitting the measurements. Nevertheless, it is not possible to avoid all physical submodels. The selection of included submodels and assumptions serves the flexibility and computational efficiency of the simulator. The submodels of physical processes used in the simulator include some innovations listed below.

Equation of the evolution and balance of small ions includes the suppression of ion concentration by ion-induced nucleation and effect of asymmetric charge of aerosol particles. The factor of depletion of ions on large particles of the pre-existing aerosol is parametrized so that the size distribution of these particles is presented through one parameter: the length of the particle chain composed from all particles in a unit volume.

It is expected that the units attaching the growing particle may be not only small inorganic molecules but also clusters of molecules or large molecules. Thus the size of the growth units is not neglected and the condensation is considered as the coagulation of growth units with growing particle. The coagulation is calculated according to the Sahni model for the transitional regime. The effect of the van der Waals forces is parametrized by adding an extra capture distance to the particle - growth unit collision distance. According to the general style of the data-fitting simulator, the van der Waals capture distance is not calculated in the simulator, but included into the set of user-controlled input parameters.

The particles can be charged or neutralized by attaching small ions. The attachment coefficients are calculated according to an approximate model that is fitted to the numerical results by Hoppel and Frick (1986) and experimental results by Reischl et al. (1996), and converges to the experimental value of the ion-ion recombination coefficient when estimating the attachment of negative ions to positive ones and vice versa. The interaction of a charged particle with non-polar growth units polarized by electrostatic induction is accounted for according to the ($\infty-4$) potential model. Two alternatives are considered for the interaction with permanent dipoles like the molecules of sulfuric acid. The first alternative is the model of the effective polarizability traditional in gaseous electronics and the second alternative is the model proposed by Nadykto and Yu (2003). The effects calculated according to two alternative models are proportional to each other, but the effect according to Nadykto and Yu is just double of the effect calculated according to the model of effective polarizability. The controversy remains unsolved and the user of the simulator is free to use any of these submodels by choosing corresponding input parameters.

The mutual coagulation of growing nanoparticles is neglected, which is a key simplification serving the computational efficiency of the model. The sink of nanoparticles includes coagulation with large particles of the pre-existing background aerosol.

The growth of particles is considered as coagulation with the two kinds of growth units that may have different parameters specified in the user-controlled input file. The growth units of the first kind (e.g. sulfuric acid) are responsible for the nucleation and slow initial growth of particles and the second (e.g. an organic substance) for quicker growth after passing the threshold size of the nano-Köhler model (Kulmala et al., 2004a). The plain kinetic growth rates are considered as the control parameters. A plain growth rate ignores the effects of the diffusion of the particles, the size of the growth units, rebound of the growth units, evaporation, and electric effects. The factors that change the growth rate are the effect of growth unit interception, diffusion of particles, transition to the continuum regime, rebound of the growth units at collisions, and thermal detachment or evaporation of condensed substance. The transition to the continuum regime is included according to the Sahni model. The rebound of growth units from the particles of diameter up to a few nanometers is calculated according to the Einstein law like in the theory of ion mobility (Tammet, 1995). The evaporation is included according to the nano-Köhler model.

Computing time on an ordinary PC is counted in seconds in case of a typical task with several thousands of time steps and several thousands of size sections. A huge number of size sections suppresses the effect of the numerical diffusion. Flexibility, convenient control of

input parameters, and the computing efficiency allow using the simulator as a practical tool when looking for the interpretation of measurements of the atmospheric aerosol nucleation bursts.

Acknowledgements. This work was supported by the Estonian Science Foundation under grant no. 4622. The authors thank Dr. M. Noppel, Dr. J. Salm, and Dr. U. Hörrak for valuable discussions.

References

- Alam, M.K. (1987) The effect of van der Waals and viscous forces on aerosol coagulation. *Aerosol Sci. Technol.*, **6**, 41-52.
- Chapman, S. & Cowling, T.G. (1970) *The mathematical theory of non-uniform gases*. Cambridge: Cambridge University Press.
- Clement, C.F., Kulmala, M., & Vesala, T. (1996) Theoretical consideration on sticking probabilities. *J. Aerosol Sci.* **27**, 869-882.
- Einstein, A. (1914) Zum gegenwärtigen Stande des Problems der spezifischen Wärme. *Abhandl. Deutsch. Bunsengesellschaft*, **3**, 330-364.
- Fuchs, N.A. (1963) On the stationary charge distribution on aerosol particles in a bipolar ionic atmosphere. *Geofis. pura e appl.*, **56**, 185-193.
- Fuchs, N.A. (1964) *The mechanics of aerosols*. London: Pergamon Press
- Fuchs, N.A. & Sutugin, A.G. (1971) High-dispersed aerosols. In: *Topics in current aerosol research*, ed. G.M. Hidy and J.R. Brock, Pergamon Press, pp. 1-60.
- Harrison, R.G. & Carslaw, K.S. (2003) Ion-aerosol cloud processes in the lower atmosphere. *Rev. Geophys.* **41**, 3/1013, doi:10.1029/2002RG000114.
- Hoppel, W.A. & Frick, G.M. (1986) Ion-aerosol attachment coefficients and steady-state charge distribution on aerosols in a bipolar ion environment. *Aerosol Sci. Technol.* **5**, 1-21.
- Huang, D.D., Seinfeld, J.H., & Marlow, W.H. (1990) BGK equation solution of coagulation for large Knudsen number aerosols with a singular attractive contact potential. *J. Colloid Interface Sci.*, **140**, 258-276.
- Hwang, N.-M., Jeon, I.-D., & Kim, D.-Y. (2000) Charged cluster model as a new paradigm of crystal growth. *J. Ceramic Processing Res.*, **1**, 34-44.
- Jacobson, M.Z. & Seinfeld, J.H. (2004) Evolution of nanoparticle size and mixing state near the point of emission. *Atmospheric Environment*, **38**, 1839-1850.
- Kerminen, V.-M. & Kulmala, M. (2002) Analytical formulae connecting the "real" and the "apparent" nucleation rate and the nuclei number concentration for atmospheric nucleation events. *J. Aerosol Sci.*, **33**, 609-622.
- Korhonen, H., Lehtinen, K.E.J., Pirjola, L., Napari, I., Vehkamäki, H., Noppel, M. & Kulmala, M. (2003) Simulation of atmospheric nucleation mode: A comparison of nucleation models and size distribution representations. *J. Geophys. Res.*, **108**(D15), 4471, doi:10.1029/2002JD003305.
- Kulmala, M., Dal Maso, M., Mäkelä, J.M., Pirjola, L., Väkevä, M., Aalto, P., Mäkeläinen, P., Hämeri, K., & O'Dowd, C.D. (2001) On the formation, growth and composition of nucleation mode particles, *Tellus*, **53B**, 479-490.
- Kulmala, M., Kerminen, V.-M., Anttila, T., Laaksonen, A. & O'Dowd, C.D. (2004a) Organic aerosol formation via sulphate cluster activation. *J. Geophys. Res.*, **109**, D04205, doi:10.1029/2003JD003961.
- Kulmala, M., Vehkamäki, H., Petäjä, T., Dal Maso M., Lauri, A., Kerminen V.-M., Birmili, W., & McMurry, P.H. (2004b) Formation and growth rates of ultrafine atmospheric particles: A review of observations. *J. Aerosol Sci.*, **35**, 143-176.

- Laakso, L., J. M. Mäkelä, L. Pirjola, and Kulmala M. (2002) Model studies on ion-induced nucleation in the atmosphere. *J. Geophys. Res.*, **107**(D20), 4427, doi:10.1029/2002JD002140.
- Lehtinen, K.E.J. & Kulmala, M. (2003) A model for particle formation and growth in the atmosphere with molecular resolution size. *Atmos. Chem. Phys.*, **3**, 1-8.
- Loeb, L.B. (1955) *Basic processes of gaseous electronics*. Berkeley and Los Angeles: University of California Press.
- Lovejoy, E.R. & Curtius, J. (2001) Cluster ion thermal decomposition (II): master equation modeling in the low-pressure limit and fall-off regions, bond energies for $\text{HSO}_2^-(\text{H}_2\text{SO}_4)_x(\text{HNO}_3)_y$. *J. Phys. Chem. A*, **105**, 10874-10883.
- Luts, A., & Salm, J. (1994) Chemical composition of small atmospheric ions near the ground. *J. Geophys. Res.* **99**, 10781-10785.
- Mason, E.A. & McDaniel, E.W. (1988) *Transport properties of ions in gases*. New York: John Wiley.
- McDaniel, E.W. & Mason, E.A. (1973) *The mobility and diffusion of ions in gases*. New York: John Wiley.
- Nadykto, A.B. & Yu, F. (2003) Uptake of neutral polar vapor molecules by charged clusters/particles: Enhancement due to the dipole-charge interaction. *J. Geophys. Res.*, **108**(D23), 4717, doi:10.1029/2003JD003664.
- Nelson, R.D. (1995) *Dispersing powders in liquids*. Amsterdam: Elsevier. (<http://www.erpt.org/024Q/Nelsb-00.htm>)
- Nelson, D., Benhenni, M., Yousfi, M., & Eichwald, O. (2001) Basic data of polyatomic ion-molecule systems for flue gas discharge modelling. *J. Phys. D: Appl. Phys.*, **34**, 3247-3255.
- Petrov, Yu.I. (1986) *Clusters and fine particles* (in Russian). Moscow: Nauka.
- Prakash, A., Bapat, A.P., & Zachariah, M.R. (2003) A simple numerical algorithm and software for solution of nucleation, surface growth, and coagulation problems. *Aerosol Sci. Technol.*, **37**, 892-898.
- Reischl, G.P., Mäkelä, J.M., Karch, R., & Nécid, J. (1996) Bipolar charging of ultrafine particles in the size range below 10 nm. *J. Aerosol Sci.*, **27**, 931-949.
- Salm, J. (1987) Combination of air ions in the case of symmetrical steady-state ionization (in Russian). *Acta comm. univ. Tartu*, **755**, 10-17.
- Svensmark, H. (1998) Influence of cosmic rays on Earth's climate. *Phys. Rev. Lett.*, **81**, 5027-5030.
- Tammet, H. (1991) Aerosol electrical density: Interpretation and principles of measurement. *Report Series in Aerosol Science, Helsinki*, **19**, 128-133.
- Tammet, H. (1995) Size and mobility of nanometer particles, clusters and ions. *J. Aerosol Sci.*, **26**, 459-475.
- Tammet, H., Kimmel, V., & Israelsson, S. (2001) Effect of atmospheric electricity on dry deposition of airborne particles from atmosphere. *Atmospheric Environment*, **35**, 3413-3419.
- Yu, F. & Turco, R.P. (2001) From molecular clusters to nanoparticles: The role of ambient ionization in tropospheric aerosol formation. *J. Geophys. Res.*, **106**, 4797-4814.